Science
AAAS

Supplementary Materials for

Oxygen imaging of hypoxic pockets in the mouse cerebral cortex

Felix R.M. Beinlich[1]*†, Antonios Asiminas[1]†, Verena Untiet[1], Zuzanna Bojarowska[1], Virginia Plá[1], Björn Sigurdsson[1], Vincenzo Timmel[2], Lukas Gehrig[2], Michael H. Graber[2], Hajime Hirase[1,3], Maiken Nedergaard[1,3]*
Corresponding authors: Felix R.M. Beinlich, felix.beinlich@sund.ku.dk; Maiken Nedergaard, nedergaard@urmc.rochester.edu

The PDF file includes:

Materials and Methods
Figs. S1 to S16
Tables S1 to S2

Other Supplementary Materials for this manuscript include the following:

Movies S1 to S4
Data S1

Materials and Methods

Animals and surgery

All experiments were conducted at the University of Copenhagen and were approved by the Danish Animal Experiments Inspectorate and overseen by the University of Copenhagen Institutional Animal Care and Use Committee (IACUC), in compliance with the European Communities Council Directive of 22 September 2010 (2010/63/EU) legislation governing the protection of animals used for scientific purposes (License number 2016-15-0201-01030 and 2020-15-0201-00483). C57BL/6JRj WT mice (Janvier) of both sexes were used in all experiments. Mice were housed in groups of 4 – 5 mice per cage in a temperature and humidity-controlled environment on a 12-hours light/dark cycle. They were fed with regular rodent chow and tap water ad libitum. Surgery was performed on 8 – 10 week old mice anesthetized with isoflurane (26675-46-7) (4 % induction, 1.5 % maintenance) or ketamine (6740-88-1)/xylazine (7361-61-7) (10 mg/ml and 1 mg/ml, respectively in 0.9 % saline, 0.1 ml/10 mg bodyweight i.p.). Body temperature was monitored throughout surgical procedures and maintained at 37°C. Data from animals presenting bleeding or a surgical injury were excluded from the analysis.

AAV injection

Virus injection was either performed locally into the brain using a stereotaxic frame or systemically via the i.v. route. Stereotaxic AAV injections were performed with a Hamilton syringe mounted to a micromanipulator (W.P.I.) at a 10-degree angle. At stereotaxic coordinates A/P: -1.97 mm, M/L: -3.0, V/D: -0.670 mm from bregma 700 nl virus at a concentration of $7x10^{12}$ vg/ml was injected at a rate of 100 nl/min. For i.v. injections $1x10^{11}$ vg were injected retro-orbitally in 0.9 % saline at a total volume of 100 µl. All viruses used are listed in Table S1. Animals were imaged 2 – 4 weeks after injection and after a craniotomy was performed.

Chronic and acute craniotomies

A head plate was glued to the skull and a craniotomy was made above the right somatosensory cortex. Unless otherwise stated, after dura removal the window was covered with 1.3 % Agarose (Type III-A, High EEO, Sigma) supplemented with 5 % furimazine (Nano-Glo® Luciferase Assay, N1110, Promega). To prevent the agarose from drying out, the agarose was covered with aCSF (135 mM Na^+, 142.8 mM Cl^-, 4.2 mM K^+, 1 mM $Ca2^+$, 0.8 mM $Mg2^+$, 10 mM Glucose, 10 mM HEPES) containing 5 % furimazine. On top of that, aCSF was sealed with a cover glass glued to the headplate with silicone (Kwick-Cast, W.P.I.). For recordings with the microelectrode the cover glass was not used. For chronic craniotomies, the window was sealed with a glass coverslip after dura removal.

In vivo oxygen calibration

For oxygen calibration of GeNL bioluminescence intensity, K/X anesthetized mice were used after acute craniotomy. Mice were fixed in a MAG-1 mouse holder (Narishige, Japan) and placed into a heat-insulation chamber (custom made, University of Copenhagen) with inlets for nosecone, exhaust tubing, and tubes for whisker stimulation via air puffs. Access to the craniotomy was

provided by a cut-out fitting the inner diameter of the head plate. The animal was provided with fresh air at defined O_2/N_2 ratio controlled by a gas mixer. The heat-insulation chamber was fitted under a macroscope (Nikon AZ100M, Nikon). Expression of GeNL was verified by mNeonGreen fluorescence (490 nm LED, pE4000, CoolLED, FITC/Cy5 dual-band filter set F56-200, AHF Analysentechnik). BLI was recorded at 1 Hz with an EMCCD camera (Andor iXon 897 Ultra, Andor) via a 1x Objective (AZ Plan Apo 1x, NA 0.1, 35 mm WD). Camera settings were set to: 1s exposure time per frame, 512 x 512pixel, EM Gain 17 MHz at 16-bit, Conversion Gain 3x, EM Gain Multiplier 300x, temperature -72°C. The AZ100M was further equipped with an AZ-TE80 trinocular tube with a sliding 1-8x magnification and a 10/90 % filter to the EMCCD. Images were collected with NIS-Elements AR (Version 5.02.00, Nikon), stored as uncompressed tiff files, and post-processed with Fiji (*59*).
A Clark-type electrode microsensor (OX-10 fast, Unisense A/S, Aarhus, Denmark) with a 90 % response time of < 0.3 s and an outside tip diameter of 8 – 12 µm (*60*) was inserted ~ 50 – 100 µm into the cortex near the GeNL expression. Previously, the electrode was calibrated by two-point calibration in air-saturated 0.9 % saline and anoxic sodium ascorbate/sodium hydroxide (0.1 M). All microsensors were connected to a Microsensor Monometer (Unisense A/S) and data recorded with UniAmp (Unisense A/S). The beginnings of the recordings were marked with a trigger signal from the camera in the UniAmp software. A micromanipulator (MP-225, WPI) was used to control the position of the microsensor in the brain.
BLI recordings were normalized to the average BLI of the first 60 seconds at normoxic conditions. Intensity changes upon O_2 concentration change were calculated as the average of the last 30 seconds of each indicated O_2 level (e.g. 30 – 60 s for 20%, 90 – 120 s for 40%) where the signal was stable. Onset time was calculated as the time from changing O_2 concentration until signal increase or decrease from baseline by normalizing the signal to the maximum within the 60 second window of the manipulation duration. Peak time was calculated as the time between changing O_2 concentration until peak of the signal within the 60 seconds of manipulation has been reached.

Whisker stimulation

Neurons in the barrel-field cortex of the right hemisphere were stimulated 10 times by a series of air puffs (5 Hz, 50 ms, 20 psi) to contralateral whisker of the mouse over a time of 10 s with a break of 50 s between each trial or in periods of 90 s with 30 s stimulation time as described before (*12*, *33*, *61*). A custom developed Matlab routine was used to calculate the mean of the whisker puff stimulation trials for each animal.

In vivo bioluminescence imaging

In vivo bioluminescence imaging was performed on K/X anesthetized or awake head-fixed mice, immobilized in a MAG-1 mouse holder or voluntarily running on a Styrofoam sphere. A self-build microscope (Cerna, Thorlabs) equipped with either a 2x (TL2X-SAP, Thorlabs) or 4x (and RMS4X-PF, Olympus) objective was used. Bioluminescence was recorded with a cooled EMCCD camera (Andor iXon Ultra 897) at 1 Hz. Camera settings were set to: 1s exposure time per frame, 512 x 512pixel, EM Gain 17 MHz at 16-bit, Conversion Gain 3x, EM Gain Multiplier 300x, temperature -72°C. In some cases an Andor iXon Ultra 888 was used instead. GeNL expression was verified by mNeonGreen fluorescence. Briefly, mNeonGreen was excited using a 470 nm LED (CoolLED pE-4000) and filtered by a dual band filter set (59904, Chroma). Emitted light was

filtered with a 500 nm (ET500LP, Chroma) long pass filter for mNeongreen emission. In cases where mNeonGreen fluorescence was used to measure if local hemoglobin absorption reflects in negative changes in fluorescence similar those seen with BLI, mNeonGreen fluorescence was recorded at 1 Hz (Andor iXon 888 Ultra, bin2, Gain 2). Images were collected with µManager (Version 2.0) (*62*), stored as 16-bit uncompressed tiff files and post-processed with Fiji (*59*).

Intrinsic Optical Spectroscopy Imaging (IOSI)

IOSI was performed on awake head-fixed mice, immobilized in a MAG-1 mouse holder. Brain tissue was illuminated by collimated (525 nm, CoolLED pE-4000) and filtered (FF01-530/11, Semrock) light directly guided to the brain surface via a bifurcated fiber (BF19Y2HS02, Thorlabs). A 2x magnification objective was used for recordings (TL2X-SAP, Thorlabs). Reflected light was filtered by a 650 nm short pass filter (FESH 650, Thorlabs) to exclude infra-red light from the observation LED (850 nm, Thorlabs) and recorded at 1 Hz (960 ms exposure time, bin 2, Andor iXon Ultra 888, Andor) with µManager. Image files were stored as 16-bit uncompressed tiff files. The camera was triggered by a Master-8 pulse generator.

Microsphere injection and in vivo macroscopic imaging

Capillary stalling was induced by i.v. injection of 4 µm microspheres (*28*). Red microspheres (4 µm, 2% solids, FluoSpheres F8859, Invitrogen) were diluted (1:5) in saline and injected i.v. after sonication via retro-orbital injection before imaging under KX anesthesia as described above. Microspheres were recorded during bioluminescent oxygen imaging utilizing the readout phase of the BLI recording camera using a self-built two camera microscope. Briefly, red microspheres were excited by 550 nm LED (pE4000, CoolLED) filtered through a 488/561 dual color filter set (59904, Chroma) and guided to the animal via a 2x objective (TL2X-SAP, Thorlabs). Emitted fluorescence was collected with an EMCCD camera (Andor iXon 888 Ultra, Andor) after passing the 488/561 dual color filter set and a 543 nm dichroic mirror (ZT543-rdc-UF1, Chroma). In parallel BLI from the oxygen probe was collected via the same optical path but recorded with a second EMCCD camera (Andor iXon 897 Ultra, Andor). Both cameras and the LED were controlled by TTL pulses coming from a Master-8 pulse generator. Images were collected with µManager (Version 2.0) (*62*), stored as 16-bit uncompressed tiff files and post-processed with Fiji (*59*).

In vivo pH measurement

After virus injection using a 10 µL glass Hamilton syringe (NF35BV-2, Nanofil, WPI) mounted to a Nanoinjector pump (Micro4, WPI), in the center of the injection site a mono fiber-optic cannula (400 µm, 0.48 NA, Doric Lenses) attached to a 2.5 mm diameter metal ferrule was implanted. A concentration of $1.8*10^{13}$ vg/mL PHP.eB AAV2 GFAP-ILP.pHuji.PTD virus was injected at stereotaxic coordinates A/P: -1.7 mm, M/L: --3.0, V/D: -0.9, -1.0.X, -1.1.X mm from bregma. Animals were imaged 2 – 4 weeks after injection.

Fiber photometry

The pH sensitive fluorescent biosensor was excited by an LED (560 nm, Tucker Davis Technologies). Together with a second LED (405 nm, Tucker Davis Technologies) used to correct for motion artifacts both were connected to a minicube (SPECS, Doric Lenses) by attenuator patch cords (400-µm core, NA = 0.48, Doric Lenses). LEDs were controlled by LED drivers Tucker Davis Technologies) and connected to RZ10-X real-time processor (Tucker-Davis Technologies). Fiber optic patch cords (400 µm core, NA = 0.48, Doric Lenses) connected the minicubes with the animals and connected via Zirconia sleeves to attach the fiber optic patch cord to fiber implants on the animal. 560 nm/405 nm excitation were sinusoidally modulated at 531 Hz/210 Hz.
Synapse (Tucker-Davis Technologies) was used to control the signal processor and collect data. Files were exported for analysis to MATLAB (MathWorks) as described before (*63*). Mice were recorded und KX anesthesia when oxygen concentration of the inhaled air was changed. For pH measurements under Hypercapnia, mice were recorded awake.
The ΔF/F calculations relied on the fitting of the 405 nm signal. To achieve normalization, the 560 nm signal and the 405 channel underwent scaling using the least-squares method, specifically utilizing the MATLAB first degree *polyfit()* function. This process determined the slope and intercept required to produce a scaled 405 nm channel. ΔF/F was obtained by subtracting the fitted control channel from the signal channel and dividing it by fitted controlled channel. Subsequently, ΔF/F was filtered with zero-phase digital filter to remove noise and down sampled by a factor of 100.

Immunohistochemistry

Mice were transcardially perfused with 20 mL 0.01 M phosphate buffered saline (PBS, pH 7.4, Sigma-Aldrich) and 20 mL of 4% paraformaldehyde solution (PFA, Sigma-Aldrich) diluted in PBS pH 7.4 under deep K/X anesthesia. The brain was harvested and post-fixed in 4% PFA overnight and sliced in 100 µm-thick coronal sections using a vibratome (VT1200S, Leica). Then, free floating immunolabelling was performed to identify the cell identity of the viral-construct infected cells. Brain sections were incubated for 1 h at room temperature in 10% normal donkey serum-PBS containing 0.1% Triton X-100 and 0.2% gelatin and 40 µg/mL AffiniPure Fab Fragment Donkey Anti-Mouse (715-007-003, Jackson Immunoresearch, UK) to suppress nonspecific binding. Primary antibodies were incubated overnight at 4C in PBS containing 5% normal donkey serum, 0.1% Triton X-100 and 0.2% gelatin followed by 3, 5-min washes in PBS. Secondary antibodies were incubated for 2 h at room temperature (1:500; Jackson ImmunoResearch; catalog 711175152 and 705175147). The specificity of the immunostaining was tested by omitting the primary antibodies (data not shown). Multichannel Z-stacks (20 µm, 1 µm step size) were acquired using the same acquisition parameters for all samples using a confocal microscope (Nikon Eclipse Ti, Tokyo, Japan).

Processing and analysis of BLI recordings

Macroscopic recordings were corrected for motion errors with the motion correction plugin of EZcalcium (*64*) and post-processed in Fiji (*59*). In addition to full field of view analysis, manually defined, rectangular (Fig. S5) or circular (Fig 2B) regions of interest were selected in the field of view and their mean traces over time were inspected.

Hypoxic Pocket detection. Hypoxic pockets were detected with custom developed Matlab routines (available at: https://doi.org/10.5281/zenodo.10629901). Briefly, after motion correction raw image files were first detrended on a pixel-by-pixel basis using a 3rd degree polynomial fit to correct for bioluminescence intensity reduction over time caused by substrate concentration decrease. To account for variability in the field of view across animals we defined the active recording tissue area. All pixels with values above the entire frame mean for at least 25% of the recording duration were defined as part of the active recording tissue area. Isolated pixels enclosed in the active recording area were also defined as part of it. The size of active recording tissue in mm^2 was used to normalize hypoxic pocket events in order to be able to compare across subjects. The detrended images were z-scored. Time traces for each pixel were z scored using following formula:

$$z = \frac{x-\mu}{\sigma} \text{ (Eq. 1)}$$

where x is the raw trace over time, μ is the mean value across time, and σ is the standard deviation of the signal over time.

The z-scored image was further filtered with a mean spatial filter with 21x21 pixel moving window. Hypoxic pockets were identified first on each frame of the smoothed imaging data, as areas with inverted signal above the 98% percentile that were part of the active recording tissue area. Based on our observations and given the absence of an existing analysis methodology, we excluded areas with less than 100 and more than 6400 pixels, and with less than 0.3 circularity score, calculated with function Matlab *regionprops(),* as:

$$circularity = \left(\frac{4*\pi*Area}{Perimeter^2}\right) * \left(1 - \frac{0.5}{r}\right)^2 \text{(Eq. 2)}$$

where *perimeter* and *Area* are the distance around the boundary of the region in pixels and number of pixels in the region respectively, and *r* is defined as:

$$r = \frac{Perimeter}{2*\pi} + 0.5 \text{ (Eq. 3)}$$

The maximum circularity value is 1 for a cycle and 0 for highly irregular areas.

Hypoxic pockets were tracked across frames based on their spatial overlap and subsequently filtered based on empirically set duration thresholds (3 s< & <150 s). Areas in the field of view found to produce hypoxic pocket events were termed regions of interest (ROIs) (see Fig 2Q-S). The mean detrended signal was extracted for each of these ROIs from the detrended image by summing pixel values for each frame, and their statistics such as area, diameter, perimeter, circularity, centroid coordinates, and signal change for individual hypoxic events they produced were calculated and correlated with other experimental parameters (e.g. movement, level of anesthesia etc.). Specifically for signal change, referred to as amplitude or $pO_2(\Delta B/B)$ in the manuscript/figures, this was calculated as signal change relative to the signal for 20 s before the hypoxic pocket event. For hypoxic events that took place within the first 20 s of recording baseline was taken as the 20 s after the end the event. To be able to compare the number of hypoxic pockets over time between different recordings/animals, the number of hypoxic pockets was normalized to a recording area of 1 mm^2 to correct for the different objectives and magnifications used. Briefly, a correction factor (κ) for each recording was determined:

$$\kappa = \frac{1000}{FOV\ \text{edge}} \text{ (Eq. 4)}$$

Where *FOV edge* is the length in µm of the square field of view of any given recording area.

Hypoxic burden. We calculated the hypoxic burden (Ξ) for each recording as a measure for the influence of hypoxic pocket parameters on tissue pO_2. First, the hypoxic burden for an individual hypoxic pocket (ξ) was defined as:

$$\xi = duration * amplitude * area \text{ (Eq. 5)}$$

Where *duration* in seconds, amplitude (pO_2(ΔB/B)) as positive signal change from baseline expressed as a fraction (e.g. 27% signal decrease during a hypoxic pocket = 0.27), and area in µm². Next, the hypoxic burden (Ξ) of a single mouse during a recording was calculated as the sum of ξ for all (n) pockets of each recording, multiplied by the correction factor (κ) to account for FOV differences, and normalized to the length of recoding in minutes:

$$\Xi = {\sum_{i=1}^{n} \xi_i * \kappa}\Big/{T_{rec}} \text{ (Eq. 6)}$$

With T_{rec} being the recording length in minute.

IOS analysis

To identify changes in IOS imaging that could resemble spatiotemporal characteristic of hypoxic pockets, the raw recordings were first inverted to account for the inverted nature of the raw IOSI signal and normalized (ΔR/R). The inverted ΔR/R image stack was then analyzed for the occurrence of hypoxic pockets with the algorithm as described above.
Hemoglobin changes within the identified hypoxic pockets was calculated as follows: We first estimated the weighted Beers-Lambert law coefficients using previously published method by Turner et al. (*65*). We used these coefficients to calculate hemoglobin concentrations and convert raw IOS imaging data. Using the masks created earlier during hypoxic pocket event identification. The relative change in hemoglobin concentration during events identified earlier was calculated by averaging the hemoglobin-estimation signal across all pixels of each event area and calculating the difference in total hemoglobin during the event duration relatively to a period of 20 s before, as previously described for BLI data.

Statistics and reproducibility

No statistical methods were used to pre-determine sample sizes. For statistical comparisons of hypoxic pocket properties between experimental conditions (e.g. KX vs awake) we used a linear mixed effects (LME) model approach to take into account the dependencies in our data (experimental conditions-mice-hypoxic pockets) and account for random effects (*66*). Statistical modelling routines for the LME models were written and run using the R package *nlme* in RStudio 2023.06.2 (Rstudio Team, 2016). *Post hoc* tests between groups were conducted by comparing

estimated marginal means with t-tests with a Tukey correction for multiple comparisons using the R package *emmeans*. One-sample t-tests were run using the R package *lmerTest* followed by correction for false discovery rate (alpha = 0.05) with Benjamini–Hochberg procedure. All other statistical compassions were conducted using GraphPad (Prism 9).

For signal correlation between FluoSpheres and ΔpO_2 signals, Pearson's correlation coefficient (r) values were transformed to (z) values. This is because r values are bounded between [− 1, 1], and the sampling distribution for highly correlated variables is highly skewed. Therefore, we converted the r value distribution to normal z value distribution using the *Fisher's* z transformation:

$$z = (0.5)\ln\frac{1+r}{1-r} \quad \text{(Eq. 7)}$$

Data and statistical analysis for all figures are provided in Data S1.

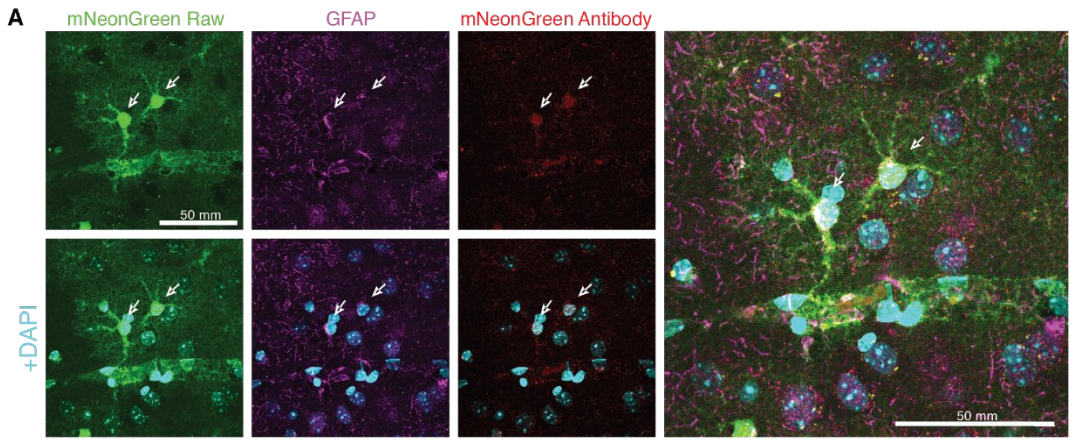

Fig. S1. Validation of cell specificity of GeNL expression. (A) Expression of GFAP-GeNL in cortical astrocytes. Overlay of mNeonGreen fluorescence (Green) with GFAP antibody staining (Purple) and mNeonGreen antibody (Red). Nuclei are labeled with DAPI (blue). Scale bars, 50 μm.

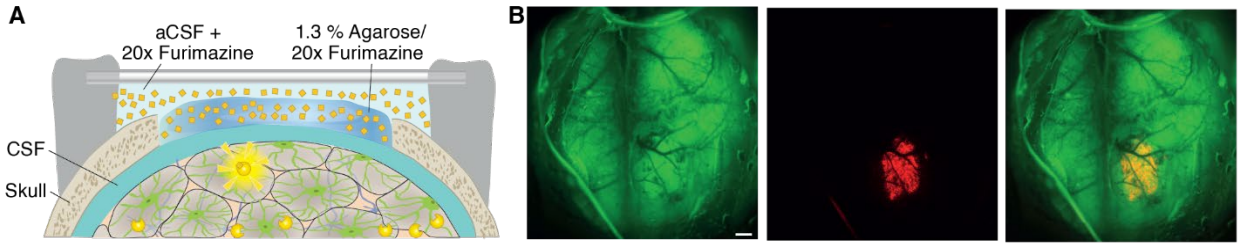

Fig. S2. Substrate administration and signal distribution. (A) Furimazine was embedded in 1.3% agarose (20x dilution) above the exposed cortex after dura removal. The agarose was covered with aCSF mixed with furimazine (20x diluted) and sealed with a cover glass to prevent auto oxidization of the substrate and to provide a reservoir of substrate for long-term recordings. **(B)** Bioluminescence intensity was limited to cranial window and area where dura has been removed. Green: Fluorescence of the sensor expressed in the whole brain after i.v. injection. Red: bioluminescence intensity. Scale bar, 500 µm.

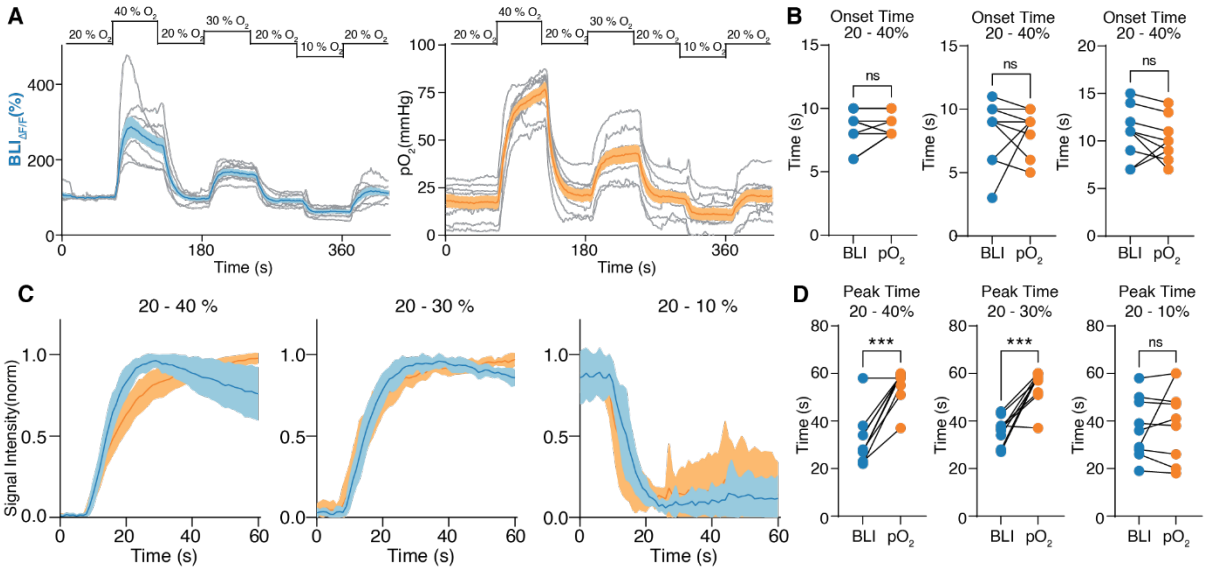

Fig. S3. Correlations of bioluminescence intensity and O2-electrode recordings during oxygen calibration. (A) Single recordings from oxygen calibration. **(B)** Comparison of onset times between BLI and electrode recordings upon oxygen change. **(C)** Onset of BLI and electrode changes upon oxygen change normalized to the maximum value within a 60 s window. Shadow indicates standard deviation (SD). **(D)** Comparison of time until peak after oxygen change at different concentrations measured with BLI and electrode recordings. Paired t test. ***: $P < 0.001$. $N = 9$ trials from 6 mice.

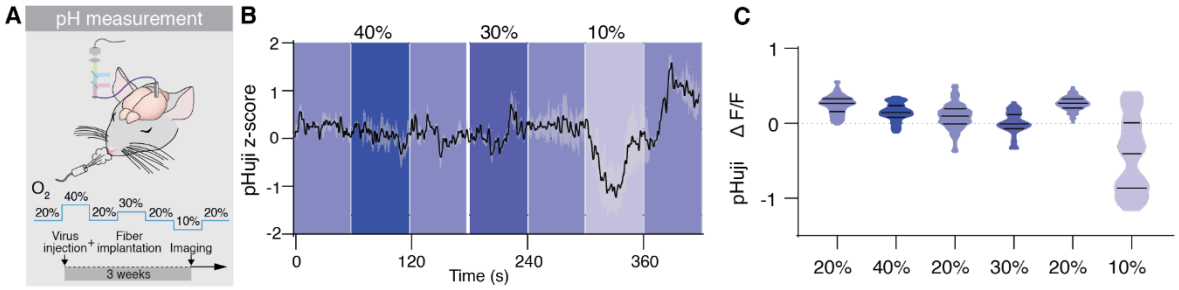

Fig. S4. Extracellular pH measurements during oxygen calibration show no relevant change. **(A)** Extracellular pH was measured in the cortex of KX anesthetized mice expressing the pHuji in the membrane of astrocytes facing the extracellular space. A fiber photometry probe was inserted, and oxygen concentration of the inhaled air was changed according to the protocol outlined. **(B)** Average trace of pH change represented as ΔF/F over time during O_2 manipulation in the tidal air. Shading indicates SEM. **(C)** Frequency distribution of pHuji ΔF/F at different O_2 levels. One-way RM ANOVA: $F_{5,\ 5492} = 417.7802$. $p<0.0001$ main effect of group (no statistically significant differences from baseline=0). $N = 3$ mice.

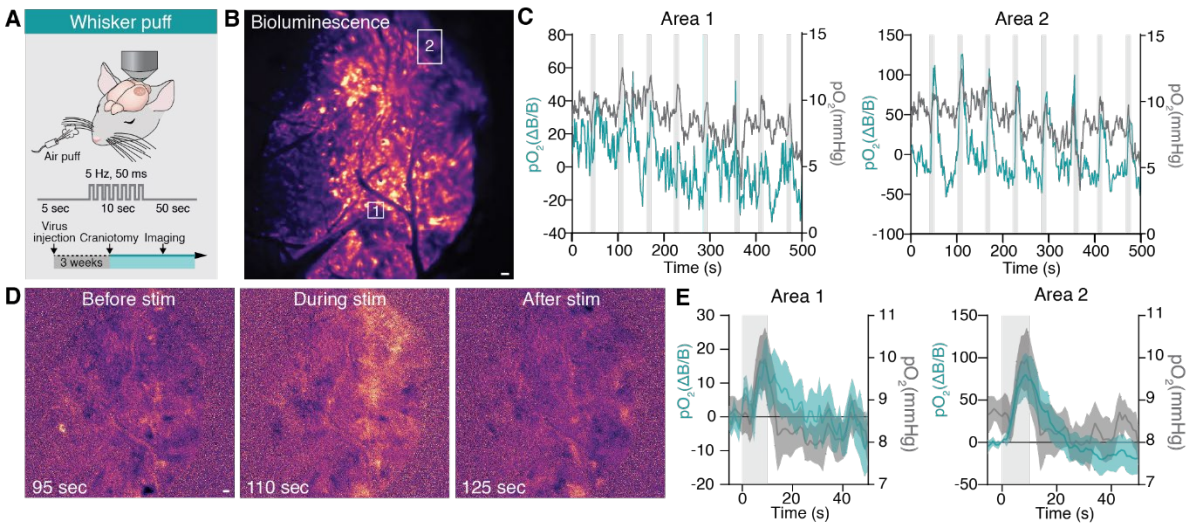

Fig. S5. Bioluminescence intensity follows O_2 electrode upon functional hyperemia. (A) Cerebral pO_2 was measured using BLI and an O_2-sensitive microelectrode in somatosensory cortex of KX anesthetized mice subjected to air-puff whisker stimulation at 5 Hz, 50 ms pulse duration, 20 psi for 10 s repeated 8 times every minute. **(B)** Average BLI distribution with indicated ROIs. **(C)** Time trace of bioluminescence intensity and O_2 electrode recordings from area 1 and 2 from **B**. **(D)** Representative images from single frames at indicated time points showing increase in BLI during whisker stimulation from **B**. Before, during, and after a series of air puffs. **(E)** Average trace of 8 repetitions of air puffs to the whiskers of ΔpO_2 measured with BLI and O_2-electrode from 2 areas indicated in D. Shading indicates SEM. Time point of whisker stimulation shown in light grey. Overall group effect $F_{2,\ 1176} = 0.0991$, $p = 0.90568$. Tukey posthocs: BLI Area 1 vs Electrode: $p = 0.9054$; BLI Area 2 vs Electrode: $p = 0.9948$. Scale bars, 100 µm.

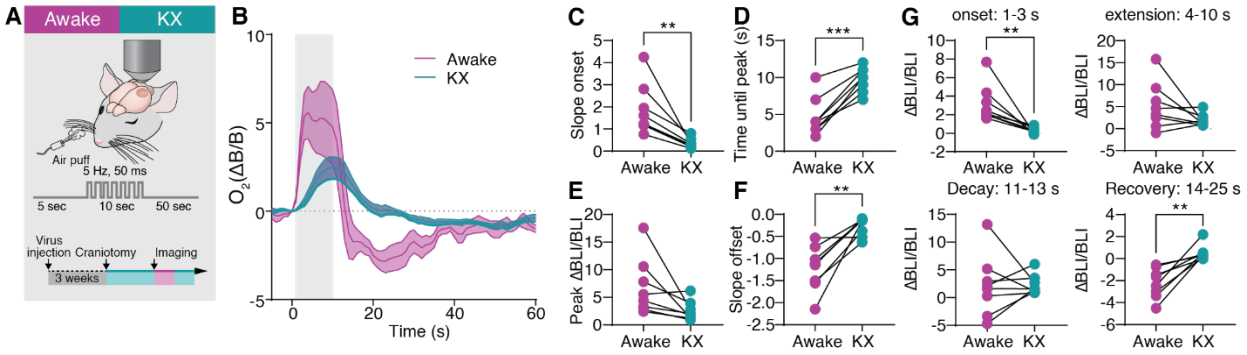

Fig. S6. Functional hyperemia is more prominent in awake mice compared to KX anesthetized mice. (A) Cerebral pO_2 during whisker stimulation was measured using bioluminescence intensity (BLI) in the cortex of KX anesthetized and awake mice subjected to air-puff whisker stimulation at 5 Hz, 50 ms pulse duration, 20 psi for 10 s repeated 8 times every minute. Mice were first measured awake followed by KX injection. **(B)** Average traces of change in BLI upon whisker stimulation over all trials. **(C)** Delay in slope onset between awake and KX mice. **(D)** Time until peak of BLI after stimulation onset. **(E)** Maximum BLI changes upon whisker stimulation. **(F)** Slope offset after whisker stimulation. **(G)** Average BLI from baseline at different time points. Upon onset (1 – 3 s), during extension time (4 – 10 s), in the decay phase after whisker puff (11 – 13 s), and in the recovery phase (14 – 25 s). Paired t test. $N = 8$ mice.

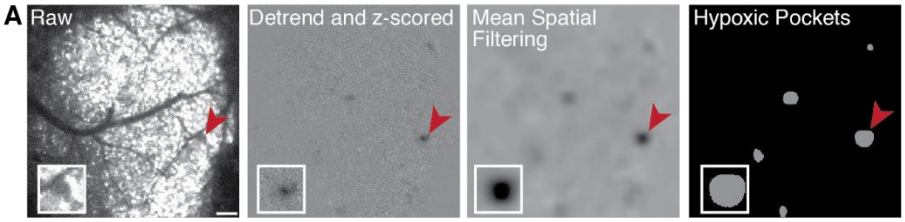

Fig. S7. Automatic detection pipeline for hypoxic pockets. (A) The raw image file is first detrended and hypoxic pockets are identified after mean spatial filtering. Scale bar: 100 µm.

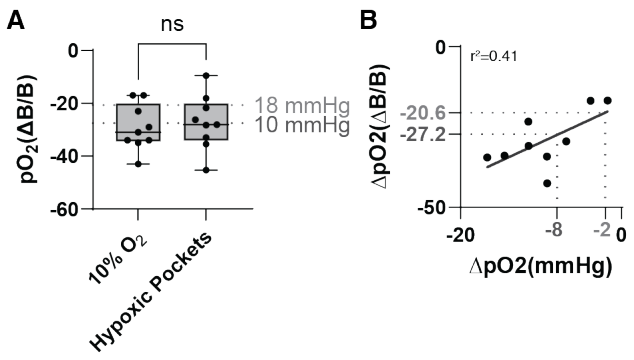

Fig. S8. Hypoxic pockets reach the hypoxic threshold. (A) Box and whisker plots showing BLI signal change [pO_2(ΔB/B)] in response to reduction of inhaled oxygen concentration to 10% as well during hypoxic pocket events in KX anesthetized mice. On average, the change corresponds approximately to 10 mmHg tissue pO_2. 18 mmHg is the previously determined hypoxic threshold. (**B**) Change in BLI and corresponding change in pO_2 recorded with the O_2 electrode in the same region upon changes in O_2 concentration of the inhalation air. This is effectively an aspect of already plotted data (Fig 2F) but focussing on hypoxia. Data points are fitted with a linear regression with an r^2 of 0.4. The x-axis corresponds to a decrease of tissue pO_2 from 20 mmHg (at 20% inhaled oxygen). A reduction of 2 mmHg equals 18 mmHg tissue pO_2, and 8 mmHg equals 10 mmHg tissue pO_2. Two-tailed unpaired t Test: p = 0.67. *N*= 9 trials from 6 mice (10% O_2) and *N* = 9 mice (Hypoxic Pockets).

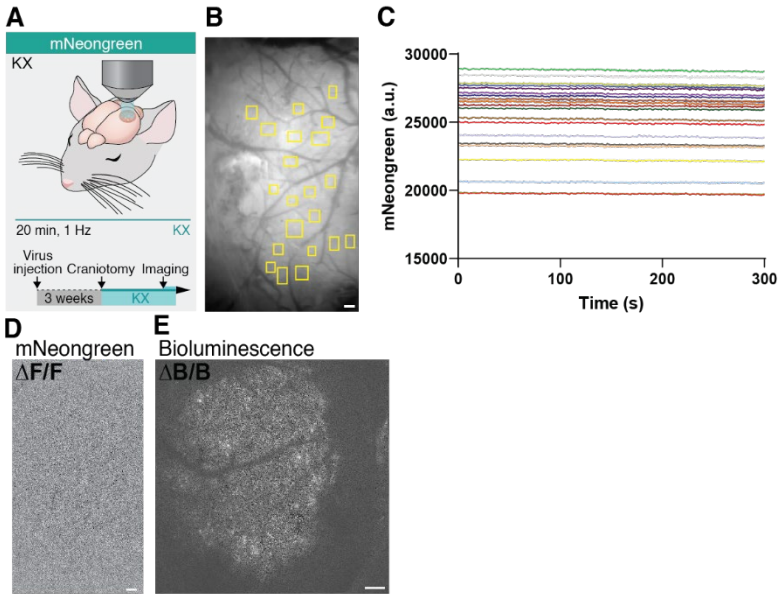

Fig. S9. mNeonGreen fluorescence is stable over time. (A) GeNL fluorescence was measured by excitation of mNeongreen with a 490 nm LED in the cortex of KX anesthetized mice after acute craniotomy and furimazine administration. **(B)** Average projection of a 300 s long recording of mNeonGreen. Yellow squares indicate manually drawn ROIs. **(C)** mNeonGreen fluorescence over time. Each trace represents a ROI from **B**. **(D)** Average projection of the ΔF/F normalized recording **B**. **(E)** Average projection of the ΔB/B normalized bioluminescence image of a representative recording (from Fig. 2B). Brighter spots indicate changes from mean intensity. Scale bars, 100 µm.

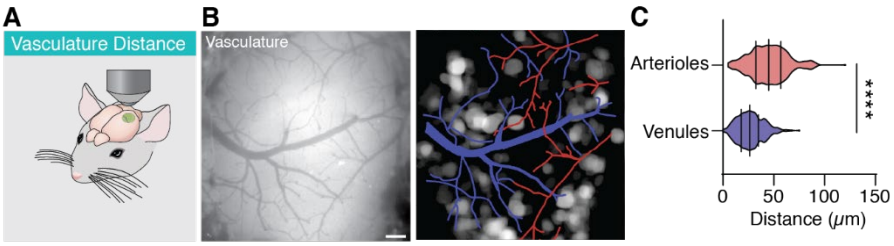

Fig. S10. Distance to vasculature. (A) Cerebral pO_2 was measured using bioluminescence intensity (BLI) in the cortex of awake mice and hypoxic pockets were identified. **(B)** Arterioles and venules were identified from white light images of the recording area, and distance to vasculature was measured from the centroid of the hypoxic pockets. **(C)** Frequency distribution of the distance of the centroid of a hypoxic pocket to the nearest arteriole and venule, respectively. One-way repeated measures ANOVA $F_{1, 3293} = 245.1$, $p<0.0001$ main effect of group. N = 8 mice. Violin plots show median and quartiles. Scale bar, 100 µm.

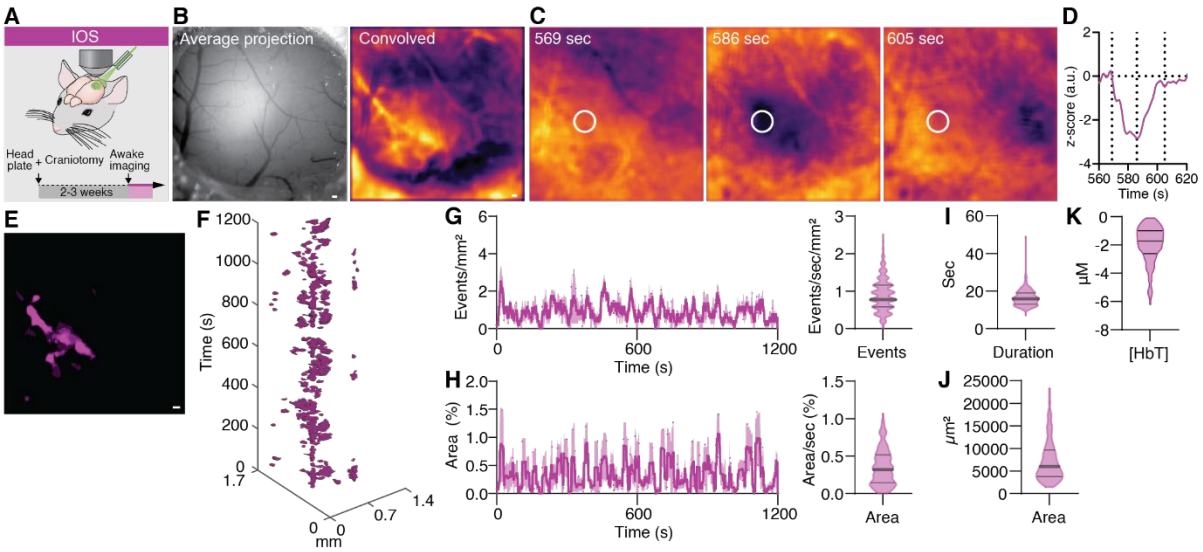

Fig. S11. Areas of low hemoglobin concentration. (A) Cerebral hemoglobin concentration ([HbT]) was imaged with intrinsic optical spectroscopy (IOS) at the isosbestic point for [HbT] in the somatosensory cortex through a cranial window in awake mice head restrained under a microscope for 20 minutes. **(B)** Left: Average projection of the reflection data of the mouse cortex illuminated with 525 nm LED. Right: Average projection after convolution of the raw reflection data. **(C)** Representative images recorded a 569, 586, and 605 s from **B. (D)** Time trace of hemoglobin concentration derived from the ROI marked in the convolved image series **C**. Dotted lines indicate timepoints from **C**. **(E)** Average projection of low flow areas from **B**. **(F)** Low flow areas detected from the IOS data in the form of regions of interest over time displayed in x-y-t 3D rendering. Lilac regions denote signal. **(G)** Average number of low flow areas per mm² detected per second. **(H)** Area covered by low flow areas per second. **(I)** Duration of low flow events**. (J**) Size of low flow areas**. (K**) Change in [HbT] during low flow events. $N = 3$ mice. Data represent mean ± SEM. SEM = standard error of the mean. Violin plots show median and quartiles. Scale bars: 100 µm.

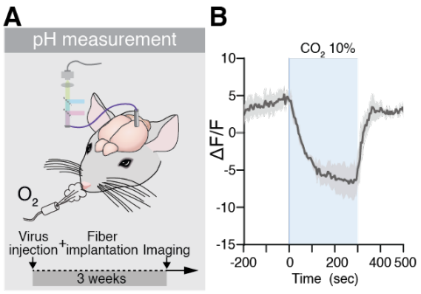

Fig. S12. Extracellular pH during hypercapnia. **(A)** Extracellular pH was measured in the cortex of KX anesthetized mice expressing pHuji in the membrane of astrocytes facing the extracellular space. A fiber photometry probe was inserted, and CO_2 concentration of the inhaled air was changed for five minutes during recording. **(B)** Time trace of the average change in pHuji fluorescence during hypercapnia (10% CO_2, blue shaded area). Data represents mean ± SEM. SEM = standard error of the mean. $N = 3$ mice.

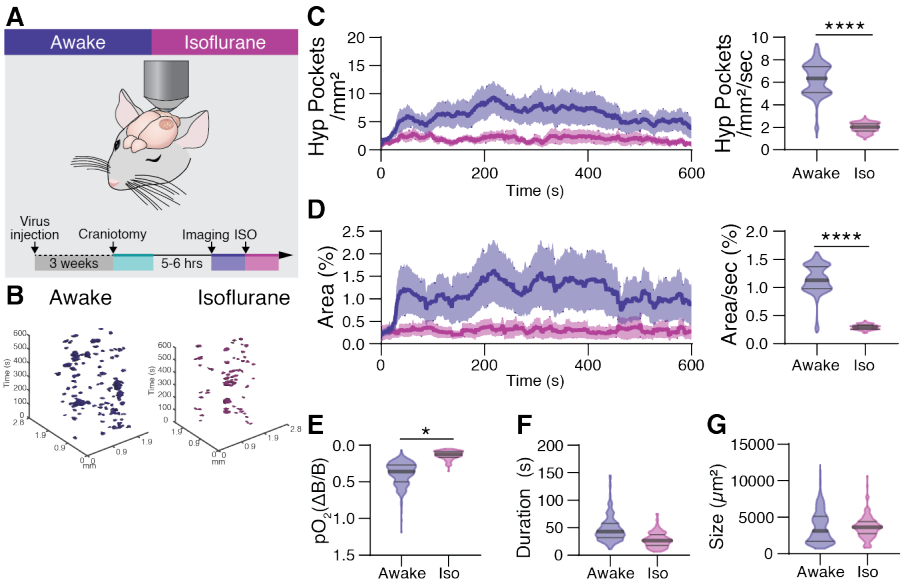

Fig. S13. Hypoxic pockets are suppressed by isoflurane-induced vasodilation. (A) Cerebral pO_2 was measured in awake head-fixed and isoflurane anesthetized mice, respectively, after acute craniotomy. First, mice were recorded for ten minutes awake followed by measurement under isoflurane anesthesia. **(B)** Hypoxic Pockets during quiet wakefulness (Left) and during isoflugrane anesthesia (right) in the form of regions of interest over time displayed in a x-y-t 3D rendering. Blue regions denote signal from awake mice, lilac regions denote signal from isoflurane anesthetized mice. **(C)** Left: Average number of hypoxic pockets per mm² during transition from normoxia to hyperoxia. Shading indicates ± SEM. Right: Number of hypoxic pockets per mm² per second. **(D)** Left: Average area covered by hypoxic pockets during transition from normoxia to hyperoxia. Shading indicates ± SEM. Right: Area covered by pockets per second. **(E)** $pO_2(\Delta B/B)$ of hypoxic pockets. **(F)** Duration of hypoxic pockets. **(G)** Size of hypoxic pockets. $N = 7$ mice; Means ± SEM are shown; SEM = standard error of the mean. Bars indicating Tukey's *post-hoc* tests between groups at their edges: *: $P < 0.05$, **: $P < 0.01$, ***: $P < 0.001$, ****: $P < 0.0001$.

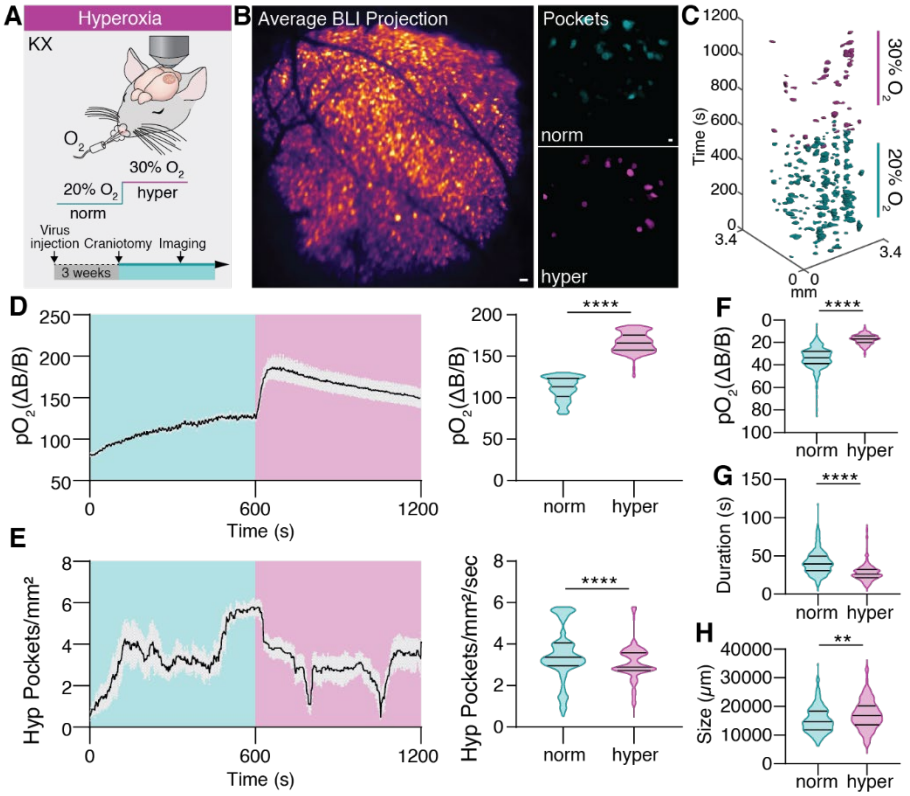

Fig. S14. High tissue oxygen diminishes hypoxic pockets. (A) Cerebral pO_2 was measured in KX anesthetized mice. Oxygen concentration in the inhaled air was increased from 20% (normoxic) to 30% (hyperoxic) for ten minutes after ten-minute baseline recording. **(B)** Left: Average bioluminescence intensity projection of a representative recording. Right: Projection of hypoxic pockets during period of normoxic (norm) and hyperoxic (hyper) conditions from the same recording. **(C)** Hypoxic pockets during the experiment in the form of regions of interest over time displayed in a x-y-t 3D rendering. Cyan regions denote signal during normoxia, lilac regions denote signal during hyperoxia. **(D)** Left: Average pO_2 traces during transition from normoxia to hyperoxia. Normalized to the first 600 s of the recording at normoxic conditions. Shading indicates ± SEM. Right: pO_2 increases by 55% during hyperoxia. One-way Repeated measures ANOVA $F_{1, 2999} = 9529.9$, $p<0.0001$ main effect of group. **(E)** Left: Average number of hypoxic pockets per mm² during transition from normoxia to hyperoxia. Shading indicates ± SEM. Right: Number of hypoxic pockets per mm² per second decreases by 11%. One-way Repeated measures ANOVA $F_{1, 2999} = 31823.44$, $p<0.0001$ main effect of group. **(F)** $pO_2(\Delta B/B)$ of hypoxic pockets. **(G)** Duration of hypoxic pockets. **(H)** Size of hypoxic pockets. In **D** and **E** data is shown as Mean ± SEM. SEM = standard error of the mean. In **D-H** violin plots show median and quartiles. Bars indicating Tukey's *post-hoc* tests between groups at their edges: *: $P < 0.05$, **: $P < 0.01$, ***: $P < 0.001$, ****: $P < 0.0001$. Scale bars, 100 µm.; $N = 5$ mice.

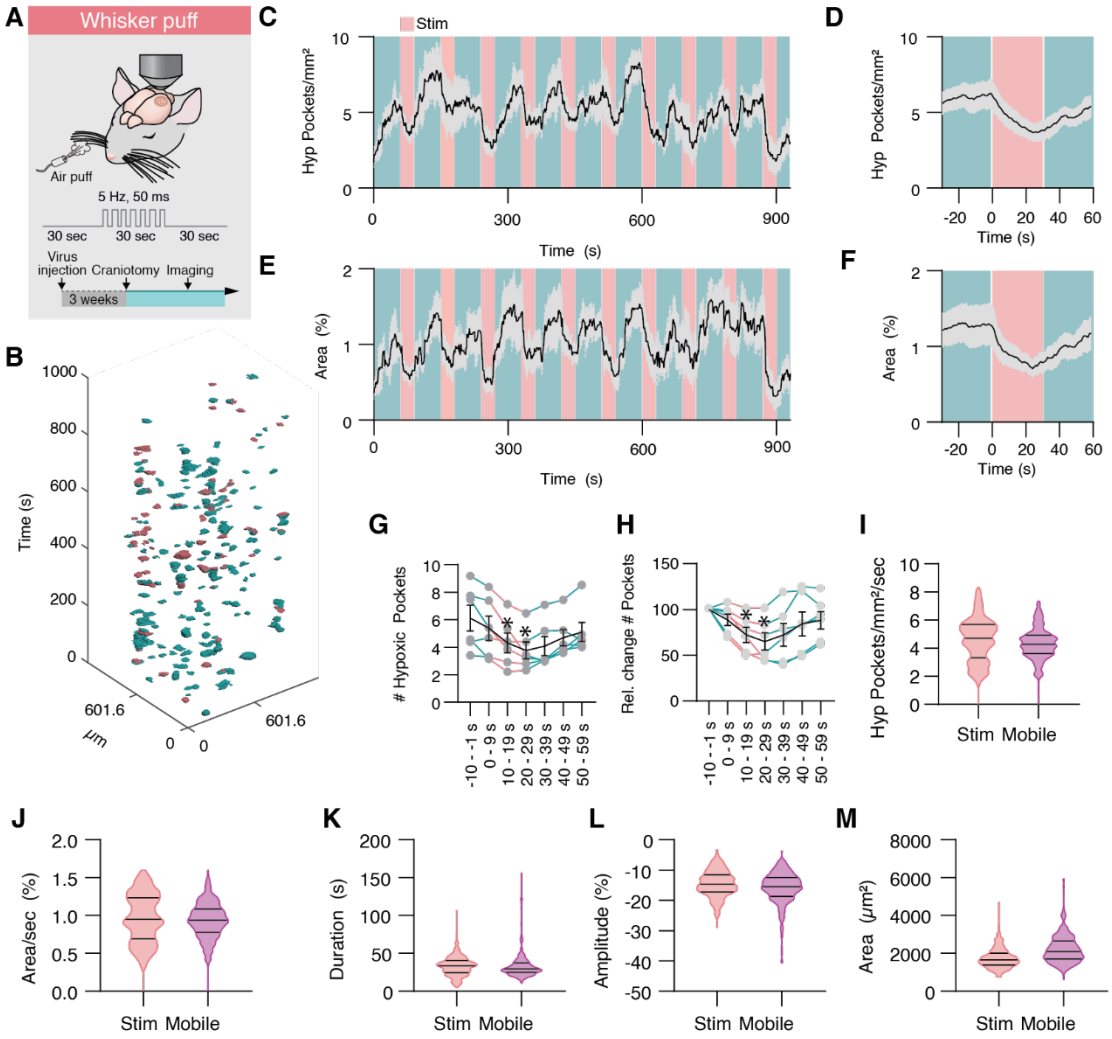

Fig. S15 Functional hyperemia reduces prevalence of hypoxic pockets. (A) Cerebral pO_2 during whisker stimulation was measured using bioluminescence intensity (BLI) in the cortex of KX anesthetized and awake mice subjected to air-puff whisker stimulation at 5 Hz, 50 ms pulse duration, 20 psi for 30 s repeated 10 times every 90 s. **(B)** Hypoxic pockets during the experiment in the form of regions of interest over time displayed in a x-y-t 3D rendering. Cyan regions denote signal during without stimulation, lilac regions denote signal during air puff administration. **(C)** Average number of hypoxic pockets per mm² during the experiment. Cyan indicates periods without stimulation. Lilac indicates periods of whisker stimulation. **(D)** Average traces of change in number of hypoxic pockets upon whisker stimulation over all trials. **(E)** Average area covered by hypoxic pockets during the experiment. **(F)** Average traces of change in area covered by hypoxic pockets upon whisker stimulation over all trials. **(G)** Change in number of hypoxic pockets in periods of 10 s. Each dot connected with a line represents a single recording. Black line with error bars (SEM) indicates average for all animals. **(F)** Change in relative number of hypoxic pockets in periods of 10 s normalized to the 10 s before stimulation onset. Each dot connected with a line represents a single recording. Black line with error bars (SEM) indicates average for all animals. **(I)** Frequency distribution of number of hypoxic pockets per second per mm² in mice exposed to functional stimulation and mobile mice. **(J)** Frequency distribution of area covered by hypoxic pockets per second in mice exposed to functional stimulation and mobile mice. **(K)**

Frequency distribution of duration of hypoxic pockets in mice exposed to functional stimulation and mobile mice. **(L)** Frequency distribution of relative pO_2 decrease of hypoxic pockets in mice exposed to functional stimulation and mobile mice. **(M)** Frequency distribution of size of hypoxic pockets in mice exposed to functional stimulation and mobile mice. Shading indicates ± SEM. SEM = standard error of the mean. Violin plots show median and quartiles. Paired t test. *: $P < 0.05$. N = 6 mice.

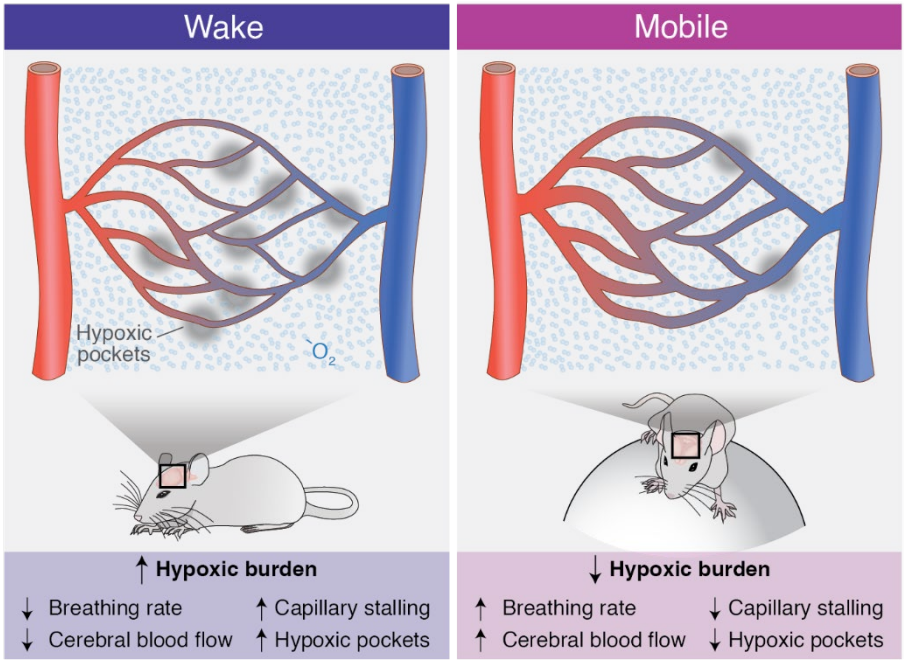

Fig. S16 Model explaining the effect of increased mobility on hypoxic pocket prevalence. (A) Left: The burden of hypoxic pockets is high during quiet wakefulness. Breathing rate and cerebral blood flow (CBF) variability are low, leading to an increase in capillary stalling and hypoxic pockets. Right: During mobile wakefulness, breathing rate (*32*) and CBF are increased, while capillary stalling and hypoxic pocket prevalence is reduced thus lowering the hypoxic burden.

Construct	Description	Company	Reference #
AAV5-GFAP(2.2)-GeNL-WPRE	Virus expressing GeNL under GFAP promoter	Vector Biolabs	**171120#19**
ssAAV-PHP.eB/2-hGFAP-GeNL-WPRE-bGHp(A)	Virus expressing GeNL under GFAP promoter in pHp.eB packaging for i.v. injection	Viral Vector Facility (VVF), Neuroscience Center Zürich	**vHH1-PHP.eB**
PHP.eB AAV2 GFAP-ILP.pHuji.PTD	Virus expressing extracellular pHuji under GFAP promoter in pH.eB. packaging for i.v. injection. GFAP-ILP.pHuji.PTD (meaning it has both Igk Leading Peptide and Pdgfr Transmembrane Domain). Outward facing pH sensor	Canadian Neurophotonics Platform Viral Vector Core	**2884**

Table S1.
List of AAV. Specifications of the virus injected.

Antigen	Immunogen	Manufacturer (CAT#)	Host & isotype	Dilution	Reference RRID#
mNeonGreen	mNeonGreen fluorescent protein derived from Branchiostoma lanceolatum	ChromoTek 32f6	Mouse/IgG2c	1:400	AB_2827566
GFAP	Glial fibrillary acidic protein (Bovine)	Agilent, Z0334	Rabbit/Ig fraction	1:500	AB_10013382
NeuN	The exact immunogen sequence used to generate this antibody is proprietary information	Abcam, ab177487	Rabbit/IgG	1:500	AB_2532109
Iba1	The exact immunogen sequence used to generate this antibody is proprietary information	Abcam, ab5076	Goat/IgG	1:500	AB_2224402

Table S2.
List of antibodies. Specifications of the antibodies used for immunohistochemistry.

Movie S1.

Change in bioluminescence intensity upon change in oxygen concentration of the inhaled air in a KX anesthetized mouse. Recorded at 1 Hz. Oxygen concentration was changed every 60 s in the following order: 20%, 40%, 20%, 30%, 20%, 10%, 20%.

Movie S2.

Change in bioluminescence intensity upon whisker stimulation in the barrel cortex of an awake mouse. Whiskers were stimulated with air puffs every 60 s beginning after 60 s for 10 s. Recorded at 1 Hz.

Movie S3.

20-minute-long recording of oxygen dynamics in the cortex of a KX anesthetized mouse. Recorded at 1 Hz.

Movie S4.

Montage of identified hypoxic pockets in a 20-minute-long recording of oxygen dynamics in the cortex of a KX anesthetized mouse. Left: raw bioluminescence intensity. Middle: Identified hypoxic pockets. Right: Overlay of hypoxic pockets and raw bioluminescence intensity. Recorded at 1 Hz.